

MOL #58289

An epilepsy-related region in the GABA_A receptor mediates long-distance effects on GABA and benzodiazepine binding sites.[†]

Marcel P. Goldschen-Ohm[†], David A. Wagner[†], Steven Petrou, and Mathew V. Jones

Department of Physiology, University of Wisconsin, Madison, Wisconsin 53706 USA (MGO, MVJ)

MOL #58289

Running Title: Long-distance effects in the GABA_A receptor.

Corresponding Author: Marcel P. Goldschen-Ohm, University of Wisconsin-Madison,
Department of Physiology, 127 SMI, 1300 University Ave., Madison, WI 53706 USA,
mpgoldschen@wisc.edu

| | |
|---------------------------------|------|
| Number of Pages | 38 |
| Number of Tables | 1 |
| Number of Figures | 7 |
| Number of References | 40 |
| Number of words in Abstract | 215 |
| Number of words in Introduction | 493 |
| Number of words in Discussion | 1474 |

MOL #58289

Abstract

The GABA_A receptor mutation γ_2 R43Q causes absence epilepsy in humans. Homology modeling suggests that γ_2 R43, γ_2 E178 and β_2 R117 participate in a salt-bridge network linking the γ_2 and β_2 subunits. Here we show that several mutations at these locations exert similar long-distance effects on other intersubunit interfaces involved in GABA and benzodiazepine binding. These mutations alter GABA evoked receptor kinetics by slowing deactivation, enhancing desensitization, or both. Kinetic modeling and nonstationary noise analysis for γ_2 R43Q reveal that these effects are due to slowed GABA unbinding and slowed recovery from desensitization. Both γ_2 R43Q and β_2 R117K also speed diazepam dissociation from the receptor's benzodiazepine binding interface, as assayed by the rate of decay of diazepam-induced potentiation of GABA evoked currents. These data demonstrate that γ_2 R43 and β_2 R117 similarly regulate the stability of both the GABA and benzodiazepine binding sites at the distant β/α and α/γ intersubunit interfaces, respectively. A simple explanation for these results is that γ_2 R43 and β_2 R117 participate in interactions between the γ_2 and β_2 subunits, disruptions of which alter the neighboring intersubunit binding sites in a similar fashion. In addition, γ_2 R43 and γ_2 E178 regulate desensitization, probably mediated within the transmembrane domains near the pore. Therefore, mutations at the γ/β intersubunit interface have specific long-distance effects that are propagated widely throughout the GABA_A receptor protein.

MOL #58289

The γ -aminobutyric acid type A (GABA_A) receptor, a member of the cys-loop superfamily of ligand-gated ion channels (LGICs), is the major mediator of inhibition in the central nervous system. The receptor is composed of five subunits arranged in a ring enclosing a central chloride ion channel. The most abundant subunits are α_1 , β_2 and γ_2 (McKernan and Whiting, 1996), which form receptors with the counterclockwise arrangement $\beta_2\alpha_1\gamma_2\beta_2\alpha_1$ when viewed from the synapse (Fig. 1A) (Baumann et al., 2002). GABA binding at the interface between β_2 and α_1 subunits triggers channel opening (Amin and Weiss, 1993; Wagner and Czajkowski, 2001), whereas binding of benzodiazepines (BZDs) such as diazepam (DZ) at the interface between α_1 and γ_2 subunits potentiates the effects of GABA (Sigel and Buhr, 1997; Boileau et al., 1998).

A third interface between the γ_2 and β_2 subunits is the site of a mutation (γ_2 R43Q) that causes childhood absence epilepsy and febrile seizures in humans (Wallace et al., 2001; Cromer et al., 2002). Similar symptoms occur in γ_2 R43Q heterozygous knock-in mice (Tan et al., 2007; and unpublished data). These mice have reduced cell surface expression of the γ_2 subunit and reduced miniature inhibitory postsynaptic currents (mIPSCs). In heterologous expression systems, the mutation alters receptor kinetics (Bowser et al., 2002; but see Bianchi et al., 2002) and impairs receptor assembly or trafficking (Kang and Macdonald, 2004; Sancar and Czajkowski, 2004; Hales et al., 2005; Frugier et al., 2007; Eugène et al., 2007). Either kinetic or trafficking effects could result in hyperexcitability and seizures: the former by accumulation of desensitized receptors during high frequency transmission, and the latter by decreasing the number of functional receptors.

Modeling based on homology with the crystallized acetylcholine binding protein suggests that γ_2 R43, γ_2 E178, and β_2 R117 participate in a salt-bridge network linking the γ_2 and β_2 subunits (Fig. 1B) (Cromer et al., 2002). This region conforms to a highly conserved motif that may mediate intersubunit communication across the LGIC superfamily (Hales et al., 2005).

MOL #58289

Interestingly, interactions linking the γ_2 and β_2 subunits are in a position to transmit their effects to multiple distant regions of the protein: either through the β_2 subunit which participates in GABA binding at the β/α interface some 30 Angstroms away, or through the γ_2 subunit which participates in BZD binding at the equally distant α/γ interface (see Fig. 1A). In addition, both β_2 and γ_2 subunits contribute to the transmembrane domains containing the channel pore and gate.

Although our observations may ultimately shed light on the role of the mutation γ_2 R43Q in epilepsy, which continues to be studied in knock-in mice (Tan et al., 2007), this study primarily addresses the biophysical implications of this and related mutations on GABA_A receptor function. Here we demonstrate that mutations at γ_2 R43, γ_2 E178 and β_2 R117 similarly alter channel gating, stabilize GABA binding and destabilize BZD binding. Therefore interactions at the γ/β interface influence specific events occurring at distant intersubunit interfaces and regions involved in channel gating.

MOL #58289

Materials and Methods

Cell Culture and Transfection

Human embryonic kidney (HEK293) cells were cultured in Minimum Essential Medium with Earle's salts (Mediatech, Inc., Herndon, VA) containing 10% bovine calf serum (Sigma-Aldrich, St. Louis, MO) in a 37°C incubator under a 5% CO₂ atmosphere. Cells were transfected using a calcium phosphate precipitation method, or with the LipofectAMINE2000™ reagent (Invitrogen, Gaithersburg, MD) using the prescribed protocol, with 1-4 µg total of either αβγ (1:1:1 ratio) or αβ (1:1 ratio) from α₁, β₂, β₂R117K, β₂R117E, γ₂, γ₂R43K, γ₂R43Q, γ₂R43E, γ₂E178K and γ₂E178Q human GABA_A receptor subunit cDNAs in vector pcDNA3.1 (Invitrogen). The mutant constructs were made using recombinant PCR, and verified by double stranded sequencing of the entire coding region. Recordings were performed 24-80 hours after transfection.

Patch Clamp Electrophysiology

Recordings from outside-out patches excised from HEK293 cells were made at room temperature using borosilicate glass pipettes filled with (in mM): 140 KCl, 10 EGTA, 2 MgATP, 20 phosphocreatine and 10 HEPES, pH 7.3, osmolarity 315 mOsm. Patches were voltage-clamped at -60 mV and placed in the stream of a multibarreled flowpipe array (Vitrodynamics, Rockaway, NJ) mounted on a piezoelectric bimorph (Morgan Electro Ceramics Inc, Bedford, OH). GABA, zinc, and diazepam were dissolved in the perfusion solution, which contained (in mM) 145 NaCl, 2.5 KCl, 2 CaCl₂, 1 MgCl₂, 10 HEPES, 4 mM Glucose, pH 7.3, osmolarity 320 mOsm adjusted with sucrose. All reagents were from Sigma-Aldrich Chemicals, St. Louis, MO. A computer-controlled constant current source (WPI, Sarasota, FL) drove the bimorph to move solution interfaces over the patch with 10-90% exchange times of <200 µs, as measured by the liquid junction current at the open pipette tip after each experiment. Junction currents were

MOL #58289

generated by altering the ionic strength with an additional 5 mM NaCl or 1% H₂O in solutions containing GABA or zinc/diazepam, respectively. Currents were low-pass filtered at 5 kHz with a four-pole Bessel filter, and digitized at a rate no less than twice the filter frequency. Data were collected using an Axopatch 200B amplifier and Digidata 1320A digitizer (Molecular Devices, Sunnyvale, CA), controlled by AxoGraph software (Axograph Scientific, Sydney, AUS) running on a Macintosh G4 (Apple Computer Inc., Cupertino, CA). Curve fitting was performed using AxoGraphX, Prism 4 (GraphPad Software Inc., San Diego, CA), or homewritten routines in either C++ or Matlab 7 (The Mathworks Inc., Natick, MA).

Statistical Analysis

Significant differences were tested using either a Student's *t*-test or one-way ANOVA with post-hoc Dunnett's test, $p < 0.05$ (Prism 4). P-values are reported in the figures, but not the text. Weighted time constants (τ_w) for biexponential fits to macroscopic kinetics (i.e. $I(t) = \sum_i a_i \exp(-t/\tau_i)$) were calculated as $\tau_w = \sum_i a_i \tau_i$, where a_i and τ_i are the fractional amplitude and time constant of the i^{th} component, I is current and t is time.

Nonstationary Variance Analysis

Nonstationary variance analysis (Sigworth, 1980) was performed on responses to repeated pulses of saturating GABA (10 mM) from which ensemble mean current (I) and variance (σ^2) were calculated at each time point. The mean current was divided into 100 equally sized bins, and the variances in each bin were averaged. Plots of binned variance versus current were fit with the equation: $\sigma^2 = iI - I^2/N$, where i is the single channel current, and N is the number of channels. Conductance was computed by dividing i by the holding potential of -60 mV. Variance resulting from slow drift (i.e., rundown or runup) was corrected by local linear fitting of the drift, calculating the variance due to this trend at each point, and subtracting this

MOL #58289

drift variance (scaled by the squared current amplitude) from the total variance before fitting. This method yields accurate estimates of i and N when tested on simulated data with drift (Wagner et al., 2004).

Kinetic Modeling

Kinetic modeling was performed with homewritten software using the Q-matrix method (Colquhoun and Hawkes, 1995). We considered two simplified models of GABA_A receptor behavior, each including two ligand binding steps, channel opening and desensitization (Fig. 4A and 4B). Although more complex models are needed to explain all of the observed macroscopic and microscopic behavior of the receptor (e.g. single channel data suggests the existence of at least three open states, whereas we include only two; Fisher and Macdonald, 1997; Keramidas and Harrison, 2008), these simpler models benefit from having fewer unconstrained parameters while still being able to describe multiple aspects of receptor behavior. The model in figure 4A has been described previously (Jones et al., 1998; Wagner et al., 2004). Because this model contains a loop that was not constrained to follow microscopic reversibility, we also explored a similar model that lacked such a loop (Fig. 4B; see supplemental data). Our overall conclusions were the same for both models (compare figures 4 and S1).

Before optimization the closing rate constants α_1 and α_2 were constrained based on the single channel open times of $\alpha_1\beta_3\gamma_{2L}$ and $\alpha_1\beta_3\gamma_{2L}R43Q$ receptors. Although $\alpha_1\beta_3\gamma_{2L}$ receptors exhibit three distinct open durations, the similarly increased fraction of openings to the two longer open states with increasing GABA concentration suggests that these openings are likely to occur from doubly liganded states (Fisher and Macdonald, 1997). Therefore, α_2 was set to the inverse of the weighted average of the two longer reported open times at 600 μ M GABA (2.7 ms), and α_1 to the inverse of the shortest open time (0.3 ms) (Fisher and Macdonald, 1997).

MOL #58289

After constraining the closing rates, the maximal open probability (P_{o-max}) was set to 0.69 based on nonstationary variance analysis (Fig. 3), and the remaining unconstrained rate constants were optimized for $\alpha_1\beta_2\gamma_2$ or $\alpha_1\beta_2\gamma_2R43Q$ receptors by fitting current responses to 2-5 ms, 500 ms and paired pulses of saturating (10 mM) GABA (paired pulse data was from Bowser et al., 2002). We then fixed d_1 and r_1 based on the initial fits so as to qualitatively reproduce the observed paired pulse data, and optimized again by simultaneously fitting current responses to both 2-5 ms and 500 ms pulses for each individual patch. We have found that simultaneous fitting of multiple protocols stressing different aspects of receptor behavior (e.g. deactivation or desensitization) is often a strong constraint for model optimization. However, responses to saturating GABA are not sensitive to the binding rates. We therefore chose to optimize $k_{\pm 1}$ and $k_{\pm 2}$ for responses to subsaturating (30 μ M) GABA (Fig. 7D-E and S3D-E), during which we kept all other rates fixed and set the peak open probability (P_o) to 0.25 based on predictions from the initial optimization (such a low peak P_o cannot be estimated by noise analysis because the data produces only the linear region of a parabola; Sigworth, 1980). Finally, we optimized the model again by simultaneously fitting current responses to both 2-5 ms and 500 ms pulses of 10 mM GABA with $k_{\pm 1}$ and $k_{\pm 2}$ now fixed to their respective mean optimized values. The results of this final round were accepted as the most reliable rate constants (Fig. 4C and S1B).

Although the closing rates α_1 and α_2 above were constrained based on data from channels containing the β_3 subunit, whereas our data is from β_2 subunit-containing receptors, we chose to use these rates initially so as to incorporate the reported reduction in mean single channel open time conferred by γ_2R43Q in 1 mM GABA (Bianchi et al., 2002) (i.e. we increased the closing rate α_2 1.5-fold for the mutant). To address whether differences in open time distributions between $\alpha_1\beta_2\gamma_2$ and $\alpha_1\beta_3\gamma_{2L}$ receptors would affect our conclusions, we repeated the modeling described above with the closing rates constrained based on the three single channel open time components reported for $\alpha_1\beta_2\gamma_2$ receptors (Keramidas and Harrison, 2008;

MOL #58289

we used open times for the most frequently observed bursting mode, M-Mode) in an analogous fashion to that for $\alpha_1\beta_3\gamma_{2L}$ receptors. Because we observed different kinetic effects for the mutation γ_2R43Q than did Bianchi and colleagues (2002), we also tested whether our conclusions depended on the speeding of the closing rate α_2 by constraining it to its wild type value. Figure S3 shows that neither constraining the closing rates based on open time distributions from $\alpha_1\beta_2\gamma_2$ receptors, nor abolishing the speeding of the doubly liganded closing rate for the mutation γ_2R43Q , affected our overall conclusions.

To fit the current traces over the diazepam (DZ) dissociation timecourse (Fig. 5), the models in figure 4A and 4B were extended to allow DZ binding/unbinding from each state (Fig. 7A and S2A, respectively). For each patch, the DZ-unbound rates were first fixed by fitting the control response to 30 μM GABA alone (the fitting procedure for these currents is described above). To test the idea that altered GABA binding/unbinding can explain all of our observed effects for DZ, all of the DZ-bound rates (x^{DZ}) were constrained to be identical to their DZ-unbound counterparts (x), except for $k_{\pm 1}^{\text{DZ}}$ and $k_{\pm 2}^{\text{DZ}}$. For the model in figure 4A, we assumed that DZ binding did not change the energy associated with a complete cycle around the loop (see supplemental data) by constraining $q^{\text{DZ}} = q k_{+2}^{\text{DZ}}/k_{+2}$ and $p^{\text{DZ}} = p k_{-2}^{\text{DZ}}/k_{-2}$. To both simplify the model and allow for GABA binding to influence BZD affinity (Sieghart, 1995; Boileau et al., 1998), we split the DZ binding and unbinding transitions into three groups: those occurring between states with no bound GABA molecule ($k_{\pm\text{DZ}}$), one bound GABA molecule ($k_{\pm\text{DZ}1}$) or two bound GABA molecules ($k_{\pm\text{DZ}2}$). For each construct, $k_{-\text{DZ}}$ was set to the inverse of the observed mean decay time constant of DZ-induced potentiation following washout (Fig. 5B-C) and $k_{+\text{DZ}}$ was approximated as $10^8 \text{ M}^{-1}\text{s}^{-1}$ by dividing $k_{-\text{DZ}}$ by the affinity constant found in radioligand binding and current potentiation experiments (Sieghart, 1995; Boileau et al., 1998). Microscopic reversibility was enforced for all loops in the model containing DZ binding steps by setting $k_{+\text{DZ}1} = k_{-\text{DZ}1} k_{+1} k_{+\text{DZ}} k_{+1}^{\text{DZ}} / (k_{-1}^{\text{DZ}} k_{-\text{DZ}} k_{+1})$ and $k_{+\text{DZ}2} = k_{-\text{DZ}2} k_{-2} k_{+\text{DZ}1} k_{+2}^{\text{DZ}} / (k_{-2}^{\text{DZ}} k_{-\text{DZ}1} k_{+2})$, in that order

MOL #58289

(Colquhoun et al., 2004). The models were then optimized to fit the series of traces illustrating the decay in potentiation by starting in the state U^{DZ} with time zero being the time of DZ washout (Fig. 7C and S2C). We reached the same overall conclusions for both the models with and without a loop (compare figures 7 and S2).

Optimization used a Nelder-Mead simplex algorithm to minimize the amplitude-weighted sum of squared errors between actual and simulated currents. In all cases, significant differences in fitted parameters between constructs were tested using a two-tailed unpaired Student's *t*-test, $p < 0.05$.

Results

Mutations to lysine or glutamine at the γ_2/β_2 subunit interface enhance desensitization, slow deactivation, or both.

Responses to rapid application of 10 mM GABA were recorded in outside-out patches from HEK293 cells transfected with either $\alpha_1\beta_2$, $\alpha_1\beta_2\gamma_2$, $\alpha_1\beta_2\gamma_2R43K$, $\alpha_1\beta_2\gamma_2R43Q$, $\alpha_1\beta_2\gamma_2R43E$, $\alpha_1\beta_2\gamma_2E178K$, $\alpha_1\beta_2\gamma_2E178Q$, $\alpha_1\beta_2R117K\gamma_2$ or $\alpha_1\beta_2R117E\gamma_2$ GABA_A receptor subunit cDNA combinations. Kinetics were characterized with biexponential fits to macroscopic deactivation following brief 2-5 ms pulses, or to desensitization during 500 ms pulses (Table 1).

Individual mutations to lysine (K) or glutamine (Q) at γ_2R43 , γ_2E178 or β_2R117 always enhanced desensitization, slowed deactivation, or both. Mutations of the γ_2 residues had qualitatively equivalent effects: lysine (γ_2R43K , γ_2E178K) conferred deeper desensitization, whereas glutamine (γ_2R43Q , γ_2E178Q) sped desensitization and slowed deactivation (Fig. 1C-D). In contrast, the β_2 subunit mutation β_2R117K slowed deactivation with little effect on desensitization (Fig. 1E).

Arginine to glutamate charge reversals in either the γ_2 or β_2 subunit (γ_2R43E , β_2R117E) essentially abolished currents in response to 10 mM GABA (peak current amplitude and fraction

MOL #58289

of patches with detectable current, $\alpha_1\beta_2\gamma_2$ R43E = 7 ± 2 pA, 4 of 12 patches; $\alpha_1\beta_2$ R117E γ_2 = 22 ± 16 pA, 2 of 9 patches). These small currents precluded kinetic analysis, but are consistent with a role for these residues in receptor assembly or trafficking (Cromer et al, 2002; Hales et al, 2005).

At least one mutation at each of γ_2 R43, γ_2 E178 or β_2 R117 slowed receptor deactivation, which is shaped in part by the GABA unbinding rate (Jones et al., 1998). Thus, despite being distant from the GABA binding site, all three residues appear to participate in regulating the stability of the GABA-bound complex. Additional evidence supporting changes in the GABA unbinding rate is presented in a later section. By similar reasoning, both γ_2 subunit residues also influence desensitization while GABA is bound.

Mutations to lysine or glutamine at the γ_2/β_2 subunit interface do not preclude γ_2 subunit incorporation into functional, surface expressed receptors.

Currents recorded from receptors containing mutations at γ_2 R43 or γ_2 E178 appear kinetically similar to currents from $\alpha_1\beta_2$ receptors in that they have slower deactivation and/or deeper desensitization than currents from $\alpha_1\beta_2\gamma_2$ receptors (Fig. 2A and compare with Fig. 1C-D). Thus, the kinetic changes conferred by these mutations could potentially reflect an impaired ability to incorporate the γ_2 subunit into functional receptors. However, because $\alpha_1\beta_2$ receptors have a smaller conductance than $\alpha_1\beta_2\gamma_2$ receptors, a mixture of the two subtypes would require a larger fraction of $\alpha_1\beta_2$ receptors for the kinetics to appear $\alpha_1\beta_2$ -like. Simulations of mixed populations of $\alpha_1\beta_2$ and $\alpha_1\beta_2\gamma_2$ receptors demonstrate that most of the receptors in the population must lack the γ_2 subunit in order for impaired γ_2 subunit incorporation to explain the observed kinetics of these mutants (Fig. 2A).

To verify that a γ_2 subunit was present in functional mutant receptors, we observed the effects of 10 μ M zinc on peak GABA-evoked responses. Currents from $\alpha_1\beta_2\gamma_2$ receptors are

MOL #58289

fairly insensitive to this concentration of zinc, whereas $\alpha_1\beta_2$ receptors are almost completely blocked (Fig. 2B-C) (% zinc block: $\alpha_1\beta_2\gamma_2 = 16 \pm 5$, $n = 14$; $\alpha_1\beta_2 = 87 \pm 2$, $n = 7$) (Hosie et al., 2003). All of the mutants were less sensitive to zinc than $\alpha_1\beta_2$ receptors, suggesting that none of the mutations precluded γ_2 subunit incorporation (Fig. 2B-C) (% zinc block: $\alpha_1\beta_2\gamma_2R43K = 31 \pm 12$, $n = 6$; $\alpha_1\beta_2\gamma_2R43Q = 9 \pm 2$, $n = 9$; $\alpha_1\beta_2\gamma_2E178K = 17 \pm 1$, $n = 4$; $\alpha_1\beta_2\gamma_2E178Q = 20 \pm 6$, $n = 7$; $\alpha_1\beta_2R117K\gamma_2 = 55 \pm 5$, $n = 6$). Zinc blocked γ_2 subunit mutants to a similar degree as $\alpha_1\beta_2\gamma_2$ receptors, further suggesting that a γ_2 subunit was present in a large fraction of these mutant receptors. This is consistent with previous reports for γ_2R43Q (Wallace et al., 2001; Bowser et al., 2002). Though the charge reversal mutant γ_2R43E did not express well in outside-out patches, sufficient current was obtained from two whole cells to suggest that this mutation severely reduces γ_2 subunit incorporation into functional receptors (% zinc block = 69 ± 16 , data not shown). Zinc block of the β_2 subunit mutant $\alpha_1\beta_2R117K\gamma_2$, however, was intermediate to that of $\alpha_1\beta_2$ and $\alpha_1\beta_2\gamma_2$, which could reflect impaired assembly with the γ_2 subunit, or alternatively, a direct effect on the receptor's interaction with zinc. However, the mutation β_2R117K also exhibited kinetics that differed the most with that expected for a simple mixture of subtypes (i.e. $\alpha_1\beta_2R117K\gamma_2$ receptors desensitized like $\alpha_1\beta_2\gamma_2$ receptors and deactivated like $\alpha_1\beta_2$ receptors; compare figures 1E and 2A).

Thus, both their kinetic profiles and zinc sensitivity demonstrate that the functional effects of mutations at γ_2R43 , γ_2E178 or β_2R117 are unlikely to be artifacts caused by assembly deficits. Additional support for this conclusion is provided by changes in the kinetics of diazepam dissociation, described in a later section.

The mutation γ_2R43Q does not alter single channel conductance or peak open probability.

MOL #58289

We used nonstationary variance analysis (Sigworth, 1980) to estimate single channel conductance (γ) and maximal open probability (P_{o-max}) of the receptor (Fig 3). Because P_{o-max} is a measure that depends on the interplay between numerous microscopic transitions, it is useful not only as a general measure of microscopic gating changes, but also as a constraint on any kinetic model of the receptor (see below).

The mutation γ_2R43Q had no effect on either the single channel conductance or maximal open probability. The estimated number of channels was lower on average for $\alpha_1\beta_2\gamma_2R43Q$ than for $\alpha_1\beta_2\gamma_2$ receptors, although patch-to-patch variability precluded significance ($\alpha_1\beta_2\gamma_2$: $\gamma = 33 \pm 2$ pS, $P_{o-max} = 0.70 \pm 0.07$, $N = 341 \pm 105$, $n = 12$; $\alpha_1\beta_2\gamma_2R43Q$: $\gamma = 30 \pm 3$ pS, $P_{o-max} = 0.68 \pm 0.06$, $N = 126 \pm 33$, $n = 7$). These results are consistent with the single channel conductances observed for $\alpha_1\beta_3\gamma_{2L}$ and $\alpha_1\beta_3\gamma_{2L}R43Q$ receptors (Bianchi et al., 2002). Since $\alpha_1\beta_2$ receptors have both lower conductance and P_{o-max} ($\alpha_1\beta_2$: $\gamma = 11$ pS, $P_{o-max} = 0.40$, Wagner et al., 2004), this result again suggests that γ_2R43Q does not significantly affect γ_2 subunit incorporation into functional receptors.

The kinetic effects of the epilepsy-related mutation γ_2R43Q are explained by fast channel closure, slow recovery from desensitization and slow unbinding.

To explore the microscopic changes underlying the macroscopic kinetic effects of γ_2R43Q , we fit responses from $\alpha_1\beta_2\gamma_2$ (16 patches) and $\alpha_1\beta_2\gamma_2R43Q$ (8 patches) receptors with a kinetic model previously shown to describe multiple aspects of neuronal and recombinant GABA_A receptor function (Fig. 4A) (Jones et al., 1998; Wagner et al., 2004). The model was optimized for individual patches by simultaneously fitting current responses to 2-5 ms and 500 ms pulses of 10 mM GABA (Fig. 4D-E left, middle; see methods). We were able to quantitatively replicate all observed effects of γ_2R43Q by incorporating three specific changes: 1) increasing the channel closing rate α_2 as reported by Bianchi et al. (2002), 2) decreasing the

MOL #58289

resensitization rate r_2 and 3) decreasing the unbinding rate of GABA from the doubly liganded state k_2 . The final rate constants (mean \pm SEM) are listed in figure 4C. The same conclusions were reached for a similar model lacking a loop (see supplemental data; Fig. S1). Also, a faster closing rate was not required to explain our macroscopic observations (Fig. S3).

These simulations suggest that a residue at the γ/β intersubunit interface (γ_2 R43) participates in regulating both the stability of the desensitized state, which probably involves transmembrane regions near the channel pore (Revah et al., 1991), and GABA unbinding from the distant β/α interface. The similar kinetic profile of mutations at γ_2 E178 suggests that this residue may play a similar role. Also, because a change in deactivation with no change in desensitization or P_{o-max} strongly suggests an effect on GABA binding/unbinding (Jones et al., 1998; Wagner et al., 2004), it is very likely that β_2 R117K slows GABA unbinding as well.

The mutations γ_2 R43Q and β_2 R117K speed diazepam dissociation from the GABA_A receptor.

Our results with kinetics and modeling strongly suggest that mutations at γ_2 R43, γ_2 E178 or β_2 R117 affect processes that occur at the β/α GABA binding site such that GABA unbinding is slowed. To test whether these mutations also influence processes that occur at the α/γ interface we examined the rate at which the BZD agonist diazepam (DZ) dissociates from the receptor. Because BZD binding requires a γ_2 subunit (Sigel and Buhr, 1997), the rate of DZ dissociation depends only on the function of γ_2 subunit-containing receptors, independent of any putative effects on γ_2 subunit incorporation.

To measure the kinetics of DZ dissociation, we pre-equilibrated receptors in 10 μ M DZ, rapidly jumped to wash solution to allow DZ to unbind, then tested the remaining degree of potentiation at various wash intervals with 20-40 ms pulses of sub-maximal (30 μ M) GABA (Fig. 5A). The degree of potentiation was expressed as a percentage of the control response without

MOL #58289

DZ pre-equilibration. Only a single pulse of GABA was delivered on any sweep, and wash intervals were interleaved to compensate for any rundown.

DZ potentiated responses from $\alpha_1\beta_2\gamma_2$, $\alpha_1\beta_2\gamma_2$ R43Q and $\alpha_1\beta_2$ R117K γ_2 receptors, confirming the ability of the mutant receptors to incorporate a γ_2 subunit, although the amount of potentiation was less for both mutants than for wild-type (% potentiation immediately following washout of DZ: $\alpha_1\beta_2\gamma_2 = 36 \pm 5$, $n = 7$; $\alpha_1\beta_2\gamma_2$ R43Q = 17 ± 5 , $n = 5$; $\alpha_1\beta_2$ R117K $\gamma_2 = 10 \pm 2$, $n = 6$). Considering our kinetics, zinc, and noise analysis data, the lesser DZ-induced potentiation of both mutants compared to wild-type is likely due to a reduction in the affinity or efficacy of DZ. However, we cannot rule out that it could be due to contamination of the current by some receptors that cannot be potentiated because they lack a γ_2 subunit.

Interestingly, the timecourse of potentiation following washout of DZ was biphasic, consisting of a fast rise (i.e., increase in potentiation) followed by a slower decay (i.e., decrease back to control amplitude) (Fig. 5B). Both mutants sped the decay phase time constant by about 2-fold (τ_{decay} (s) of DZ potentiation: $\alpha_1\beta_2\gamma_2 = 3.2 \pm 0.3$, $n = 7$; $\alpha_1\beta_2\gamma_2$ R43Q = 1.8 ± 0.5 , $n = 5$; $\alpha_1\beta_2$ R117K $\gamma_2 = 1.4 \pm 0.4$, $n = 6$). The biphasic timecourse of potentiation following washout of DZ suggests two distinct transitions. The initial increase in potentiation may reflect rapid DZ unbinding from a low affinity blocking site whose occupancy counteracts potentiation caused by occupancy of a higher affinity site. Consistent with this idea, the fractional amplitude of the rising phase was reduced by $74 \pm 14\%$ ($n = 8$) following pre-equilibration in lower concentrations (1-100 nM) of DZ (data not shown). Also, previous studies have shown that BZD effects on single channel properties (e.g. opening frequency) and macroscopic kinetics (e.g., peak current potentiation) decrease at higher BZD concentrations (Rogers et al., 1994; Perrais and Ropert, 1999; Baur et al., 2008). In contrast, the slow monoexponential decay of potentiation suggests a single transition from a high affinity DZ-bound potentiated state to an unpotentiated state. The simplest interpretation is that this component reflects the dissociation of DZ from a single high

MOL #58289

affinity potentiating site, with a dissociation rate equal to the inverse of the potentiation decay time constant ($k_{-DZ} = 1/\tau_{\text{decay}}$). However, we cannot rule out more complicated interpretations, such as the existence of multiple kinetic steps between potentiation and dissociation that allow for a slow transition from potentiated to unpotentiated states while DZ is bound. In either case, the faster decay of potentiation demonstrates that the mutations have altered the function of γ_2 subunit-containing receptors, and destabilized the DZ-bound state of the receptor.

These data show that mutations at the γ/β intersubunit interface not only regulate the stability of the GABA binding site at the β/α interface, but also that of the BZD binding site at the α/γ interface.

The effects of diazepam are explained by faster GABA binding and slower unbinding.

Both $\alpha_1\beta_2\gamma_2$ R43Q and $\alpha_1\beta_2$ R117K γ_2 had faster 20-80% rise times (τ_{rise}) and slower deactivation (τ_{deact}) than $\alpha_1\beta_2\gamma_2$ receptors in response to 30 μ M GABA (Fig. 6) ($\alpha_1\beta_2\gamma_2$: $\tau_{\text{rise}} = 8.1 \pm 0.3$ ms, $\tau_{\text{deact}} = 90 \pm 8$ ms, $n = 14$; $\alpha_1\beta_2\gamma_2$ R43Q: $\tau_{\text{rise}} = 6.1 \pm 1.3$ ms, $\tau_{\text{deact}} = 141 \pm 21$ ms, $n = 4$; $\alpha_1\beta_2$ R117K γ_2 : $\tau_{\text{rise}} = 5.5 \pm 0.8$ ms, $\tau_{\text{deact}} = 148 \pm 14$ ms, $n = 11$). In addition to potentiating the amplitude of these responses, DZ sped their rise times and prolonged their deactivation, although the faster rise was not significant for γ_2 R43Q (Fig. 6). In addition, DZ did not potentiate the amplitude of responses from $\alpha_1\beta_2\gamma_2$ receptors to higher (100 μ M) GABA concentrations, but did prolong deactivation (two patches, data not shown). These results are consistent with previous studies on the effects of BZDs (Segal and Barker, 1984; Lavoie and Twyman, 1996; Mellor and Randall, 1997; Perrais and Ropert, 1999; Mercik et al., 2007) that suggest DZ mainly modulates GABA binding and unbinding rates.

To examine whether or not our observed kinetic effects of DZ could be attributed entirely to changes in GABA binding and unbinding, we fit the traces shown in figure 5A using an extension of the model in figure 4A where DZ was allowed to bind and unbind from each of the

MOL #58289

original states (Fig. 7A). For both $\alpha_1\beta_2\gamma_2$ (5 patches) and $\alpha_1\beta_2\gamma_2$ R43Q (3 patches) receptors, our data were well described by allowing DZ to modulate only GABA binding and unbinding rates (see methods). The DZ binding and unbinding rates, and the DZ-induced fold change in GABA binding and unbinding rate constants (mean \pm SEM), are listed in figure 7B. For $\alpha_1\beta_2\gamma_2$ receptors, DZ primarily sped binding of the first GABA molecule (k_{+1}), whereas for $\alpha_1\beta_2\gamma_2$ R43Q receptors binding of the second GABA molecule was increased the most (k_{+2}). For both constructs, DZ slowed unbinding largely from the doubly liganded state (k_{-2}). The differential effects of DZ on binding/unbinding of the first or second GABA molecule could reflect a preferential interaction between the DZ binding site and one of the two GABA binding sites, or altered cooperativity between GABA binding sites. In addition, the model in figure 7B predicts that the affinity for DZ should increase sequentially with GABA binding. This is consistent with the observed increase in BZD radioligand binding affinity with increasing GABA concentration (Sieghart, 1995; Boileau et al., 1998). The same conclusions were reached for a similar model lacking a loop (see supplemental data; Fig. S2).

To address whether or not our observations could be explained by DZ-induced gating changes (Downing et al., 2005; Rüsçh and Forman, 2005; Campo-Soria et al., 2006) instead of changes to GABA binding/unbinding, we refit the DZ unbinding timecourse for $\alpha_1\beta_2\gamma_2$ receptors using the model in figure 7A and allowing only the DZ-bound channel opening rates β_1 and β_2 to vary ($k_{\pm 1}$ and $k_{\pm 2}$ were constrained to be equal to their DZ-unbound counterparts). Although DZ-modulation of β_1 and β_2 was able to describe the decay in potentiation of the peak current amplitudes, we were unable to simulate the speeding of the rising phase to the degree observed (not shown), similar to the conclusion reached by Lavoie and Twyman (1996) for a much simpler kinetic scheme. Thus, for the models in figures 7A and S2A, modulation of GABA binding/unbinding rates was necessary to explain all of our observed effects of DZ on detailed nonequilibrium kinetics of both $\alpha_1\beta_2\gamma_2$ and $\alpha_1\beta_2\gamma_2$ R43Q receptors, including the timecourse of the

MOL #58289

decay in potentiation, speeding of the rising phase for $\alpha_1\beta_2\gamma_2$ receptors, and prolongation of deactivation. However, it is possible that the mutation γ_2 R43Q could confer both binding and gating effects. Indeed, when we let all of the DZ-bound rates vary except for the channel closing rates (channel open times have been shown to not depend on DZ; Vicini et al., 1987; Rogers et al., 1994), we found that although the GABA binding and unbinding rates were affected the most, the singly liganded opening rate β_1 was also increased (Fig. S2B).

MOL #58289

Discussion

There is some discrepancy regarding the effects of the epilepsy-related mutation γ_2 R43Q. Bowser et al. (2002) reported similar kinetic alterations to those shown here, whereas Bianchi et al. (2002) found no changes in macroscopic kinetics, although they did observe a reduction in mean single channel open time. Despite differences in methodology, such as whether β_2 or β_3 subunits were used, the explanation for the qualitatively different results remains unclear. However, our demonstration here of similar kinetic effects of multiple mutations clearly shows that γ_2 R43 and other residues at the γ_2/β_2 interface do indeed regulate the kinetics of $\alpha_1\beta_2\gamma_2$ receptors.

Structural interactions at the γ/β intersubunit interface.

The similarity in effects of mutations at γ_2 R43, γ_2 E178 or β_2 R117 (i.e. desensitization was enhanced or not, but never reduced, deactivation was slowed or not, but never sped, and DZ dissociation was sped for the two mutations tested) suggests that these residues are similarly involved in these kinetic processes. However, we cannot prove or disprove the existence of the specific salt-bridge network proposed by Cromer et al. (2002). Indeed, the prototypical mutant cycle analysis experiment (Carter et al., 1984), which involves the mutation of two residues to determine their interaction energy, is difficult to interpret in a three-residue network because mutating any of the residues may alter the interactions between the other two residues. Despite this, our data do illustrate the importance of charge at these positions in receptor function (and possibly assembly/trafficking), and indicate that an arginine specifically is needed for normal function at γ_2 R43 and β_2 R117. For example, reversing the charge of either native arginine (γ_2 R43E, β_2 R117E) drastically reduced currents in outside-out patches, suggesting that a non-negative charge is needed at both of these locations for either normal function or assembly/trafficking. However, the charge conserving arginine to lysine mutations γ_2 R43K and

MOL #58289

β_2 R117K both altered receptor kinetics, demonstrating that positive charge alone is not sufficient for normal function. This could be because lysine, whose side chain is slightly shorter than that of arginine, cannot position itself correctly. Lysine also has a different charge distribution than arginine, which could influence electrostatic interactions with nearby residues. Because neutralizing or reversing the charge of the central link in the putative salt-bridge network (γ_2 E178Q, γ_2 E178K) did not greatly impact current amplitudes, this residue may not play a large role in assembly/trafficking, but kinetic changes show that it does regulate the function of fully assembled channels.

Functional mutant receptors containing a γ_2 subunit.

Immunofluorescence studies have shown that mutation of γ_2 R43 to glutamine, lysine or alanine impairs surface expression of the γ_2 subunit, probably by trapping it in the endoplasmic reticulum (Kang and Macdonald, 2004; Sancar and Czajkowski, 2004; Frugier et al., 2007; Tan et al., 2007; Eugène et al., 2007). It remains unclear whether the reduced γ_2 subunit expression reflects the loss of all the constituent subunits in those receptors, such as would occur if the trapped γ_2 subunits were part of fully assembled channels (Kang and Macdonald, 2004; Hales et al., 2005), or whether the removal of γ_2 leaves behind $\alpha_1\beta_2$ receptors (Sancar and Czajkowski, 2004; Frugier et al., 2007; Tan et al., 2007). However, methods such as immunofluorescence labeling or radioligand binding cannot distinguish between a reduction in functional versus non-functional receptors. We show here that 1) all of the lysine and glutamine mutants exhibit kinetics and zinc sensitivity that are inconsistent with a simple mixture of $\alpha_1\beta_2$ and $\alpha_1\beta_2\gamma_2$ receptors, 2) γ_2 R43Q has a similar single channel conductance and P_{o-max} to that of $\alpha_1\beta_2\gamma_2$ receptors, and 3) both γ_2 R43Q and β_2 R117K alter the dissociation rate of DZ (a measure that absolutely requires the presence of a γ_2 subunit). Therefore, the responses we studied here mainly reflect receptors that contained a γ_2 subunit. These results are not incompatible with an

MOL #58289

overall reduction in the total number of surface-expressed functional receptors. Indeed, we did observe a (non-significant) trend towards reduction in the average number of channels present in patches from cells transfected with $\alpha_1\beta_2\gamma_2R43Q$ versus $\alpha_1\beta_2\gamma_2$ subunits as determined by noise analysis. Together with the arguments presented above, these data demonstrate that γ_2R43Q can assemble with α_1 and β_2 subunits. If the mutation affects trafficking it appears to impair expression of the entire $\alpha_1\beta_2\gamma_2R43Q$ complex, without leaving behind a significant number of $\alpha_1\beta_2$ receptors.

In addition to GABA-evoked macroscopic kinetics, there is also some discrepancy about the effect of γ_2R43Q on allosteric modulation by benzodiazepines. Four separate studies found that 1-2 μM DZ either did not potentiate GABA responses from mutant receptors (Wallace et al., 2001), potentiated them less than wild-type (Bowser et al., 2002; Eugène et al., 2007), or potentiated them as much as wild-type (Bianchi et al., 2002). Here we show that both $\alpha_1\beta_2\gamma_2R43Q$ and $\alpha_1\beta_2R117K\gamma_2$ form functional receptors containing the γ_2 subunit whose GABA-evoked responses are potentiated by DZ, although to a lesser degree than $\alpha_1\beta_2\gamma_2$ receptors (Fig 5). If, as our data suggest, a γ_2 subunit is present in most of the functional mutant receptors, then their reduced DZ potentiation implies either reduced affinity or efficacy of DZ. A reduction in affinity is also consistent with the observed faster dissociation of DZ from $\alpha_1\beta_2\gamma_2R43Q$ and $\alpha_1\beta_2R117K\gamma_2$ receptors.

Cooperativity between GABA binding sites.

Although we initially modeled the GABA binding/unbinding steps as being equal and independent, we were unable to reasonably fit the macroscopic responses of $\alpha_1\beta_2\gamma_2$ receptors to both 2-5 ms and 500 ms pulses of 10 mM GABA with the models in figure 4A and 4B (data not shown). We obtained good fits, however, when we allowed the individual GABA binding and unbinding steps to vary independently, such that the unbinding rates exhibited an apparent

MOL #58289

negative cooperativity ($k_{-2} > k_{-1}$), due to the rapid initial deactivation of our macroscopic responses. Although our motivation for allowing the binding and unbinding rates from the singly and doubly liganded states to vary independently was primarily to best fit the data, there is evidence that either cooperativity exists between GABA binding sites, or the sites are inherently unequal (Lavoie and Twyman, 1996; Baumann et al., 2003; Mozrzymas et al., 2003). However, a more direct model-independent measure of microscopic binding and unbinding rates is likely required to resolve this issue.

Interactions at the γ/β intersubunit interface mediate the stability of both GABA and BZD binding sites.

We show here that perturbations at the γ/β intersubunit interface are propagated to the distant ligand binding β/α and α/γ interfaces, and to regions involved in desensitization. For each of the three residues studied we found a mutation that slowed deactivation (γ_2 R43Q, γ_2 E178Q, β_2 R117K). Kinetic modeling suggests that this is due to stabilizing the GABA-bound complex. Both arginine mutations γ_2 R43Q and β_2 R117K also destabilized the DZ-bound and potentiated complex. Therefore, all three residues (γ_2 R43, γ_2 E178, β_2 R117) participate in communication between the γ/β intersubunit interface at which they reside and the GABA binding site at the β/α interface, and at least two of these residues (γ_2 R43 and β_2 R117) are also involved in communication with the BZD binding site at the α/γ interface. Assuming a counterclockwise subunit arrangement of $\beta_2\alpha_1\gamma_2\beta_2\alpha_1$ (Baumann et al., 2002), the most direct path for the propagation of structural changes between γ_2 R43 and the neighboring GABA binding site is across the γ_2/β_2 interface and through the β_2 subunit (see Fig. 1A). Similarly, the most direct path from β_2 R117 to the neighboring BZD binding site is in the opposite direction across the γ_2/β_2 interface and through the γ_2 subunit. Interestingly, if γ_2 R43, γ_2 E178 and β_2 R117 interact, then γ_2 E178 is in a position to transmit perturbations along its backbone β -strand into

MOL #58289

loop F, which has been implicated in BZD efficacy (Hanson and Czajkowski, 2008). Thus, a simple explanation for the effects of the mutations γ_2 R43Q and β_2 R117K on both GABA unbinding and DZ dissociation is that γ_2 R43 and β_2 R117 participate in interactions between the γ_2 and β_2 subunits that mediate ligand affinities at the two neighboring β/α and α/γ intersubunit interfaces. If interactions between subunits at one interface influence the structure of other intersubunit interfaces, then communication between these interfaces offers a robust mechanism for GABA or BZD binding to confer widespread conformational changes that may be important for receptor function. Indeed, both radioligand binding studies (Seighart, 1995; Bolieau et al., 1998) and our results show that DZ binding at the α/γ interface modulates GABA binding at the β/α interface, and vice versa.

We conclude that the region surrounding the epilepsy-related mutation γ_2 R43, including residues from both the γ_2 and β_2 subunits, participates in regulating events in the GABA_A receptor that are known to occur at distant regions of the protein. Kinetic analysis revealed that changes in only a few out of many possible transitions account for all of our observed effects. Therefore, perturbations at the γ/β interface affect specific locations throughout the receptor, including ligand binding sites at two separate intersubunit interfaces and the channel gating apparatus in the transmembrane domains.

MOL #58289

References

Amin J, Weiss DS (1993) GABA_A receptor needs two homologous domains of the β -subunit for activation by GABA but not by pentobarbital. *Nature* **366**: 565-569.

Baumann SW, Baur R, Sigel E (2002) Forced subunit assembly in $\alpha_1\beta_2\gamma_2$ GABA_A receptors. Insight into the absolute arrangement. *J Biol Chem* **277**: 46020-46025.

Baumann SW, Baur R, Sigel E (2003) Individual properties of the two functional agonist sites in GABA_A receptors. *J Neurosci* **23**: 11158-11166.

Baur R, Tan KR, Lüscher BP, Gonthier A, Goeldner M, Sigel E (2008) Covalent modification of GABA_A receptor isoforms by a diazepam analogue provides evidence for a novel benzodiazepine binding site that prevents modulation by these drugs. *J Neurochem* **106**: 2353-2363.

Bianchi MT, Song L, Zhang H, Macdonald RL (2002) Two different mechanisms of disinhibition produced by GABA_A receptor mutations linked to epilepsy in humans. *J Neurosci* **22**: 5321-5327.

Boileau AJ, Kucken AM, Evers AR, Czajkowski C (1998) Molecular dissection of benzodiazepine binding and allosteric coupling using chimeric γ -aminobutyric acid_A receptor subunits. *Mol Pharmacol* **53**: 295-303.

Bowser DN, Wagner DA, Czajkowski C, Cromer BA, Parker MW, Wallace RH, Harkin LA, Mulley JC, Marini C, Berkovic SF, Williams DA, Jones MV, Petrou S (2002) Altered kinetics and

MOL #58289

benzodiazepine sensitivity of a GABA_A receptor subunit mutation [γ_2 (R43Q)] found in human epilepsy. *PNAS* **99**: 15170-15175.

Campo-Soria C, Chang Y, Weiss DS (2006) Mechanism of action of benzodiazepines on GABA(A) receptors. *Br J Pharmacol* **148**: 984990.

Carter PJ, Winter G, Wilkinson AJ, Fersht AR (1984) The use of double mutants to detect structural changes in the active site of tyrosyl-tRNA synthetase (*Bacillus stearothermophilus*). *Cell* **38**: 835-840.

Colquhoun D, Hawkes AG (1995) A Q-matrix cookbook. How to write only one program to calculate the single-channel and macroscopic predictions for any kinetic mechanism, in *Single-Channel Recording* (Sakmann B, Neher E eds) pp 589-633, 2nd ed. Plenum Press, New York.

Colquhoun D, Dowsland KA, Beato M, Plested AJR (2004) How to impose microscopic reversibility in complex reaction mechanisms. *Biophys J* **86**: 3510-3518.

Cromer BA, Morton CJ, Parker MW (2002) Anxiety over GABA_A receptor structure relieved by AChBP. *Trends Biochem Sci* **27**: 89-96.

Downing SS, Lee YT, Farb DH, Gibbs TT (2005) Benzodiazepine modulation of partial agonist efficacy and spontaneously active GABA_A receptors supports an allosteric model of modulation. *Br J Pharmacol* **145**: 894-906.

MOL #58289

Eugène E, Depienne C, Baulac S, Baulac M, Fritschy JM, Le Guern E, Miles R, Poncer JC (2007) GABA_A receptor γ 2 subunit mutations linked to human epileptic syndromes differentially affect phasic and tonic inhibition. *J Neurosci* **27**: 14108-14116.

Fisher JL, Macdonald RL (1997) Single channel properties of recombinant GABA_A receptors containing γ 2 or δ subtypes expressed with α 1 and β 3 subtypes in mouse L929 cells. *J Physiol* **505**: 283-297.

Frugier G, Coussen F, Giraud M, Odessa M, Emerit MB, Boué-Grabot E, Garret M (2007) A γ 2(R43Q) mutation, linked to epilepsy in humans, alters GABA_A receptor assembly and modifies subunit composition on the cell surface. *J Biol Chem* **282**: 3819-3828.

Hales TG, Tang H, Bollan KA, Johnson SJ, King DP, McDonald NA, Cheng A, Connolly CN (2005) The epilepsy mutation γ 2(R43Q) disrupts a highly conserved inter-subunit contact site, perturbing the biogenesis of GABA_A receptors. *Mol Cell Neurosci* **29**: 120-127.

Hanson SM, Czajkowski C (2008) Structural mechanisms underlying benzodiazepine modulation of the GABA_A receptor. *J Neurosci* **28**: 3490-3499.

Hosie AM, Dunne EL, Harvey RJ, Smart TG (2003) Zinc-mediated inhibition of GABA_A receptors: discrete binding sites underlie subtype specificity. *Nat Neurosci* **6**: 362-369.

Jones MV, Sahara Y, Dzuby JA, Westbrook GL (1998) Defining affinity with the GABA_A receptor. *J Neurosci* **18**: 8590-8604.

MOL #58289

Kang J, Macdonald RL (2004) The GABA_A receptor $\gamma 2$ subunit R43Q mutation linked to childhood absence epilepsy and febrile seizures causes retention of $\alpha 1\beta 2\gamma 2S$ receptors in the endoplasmic reticulum. *J Neurosci* **24**: 8672-8677.

Keramidas A, Harrison NL (2008) Agonist-dependent single channel current and gating in $\alpha 4\beta 2\delta$ and $\alpha 1\beta 2\gamma 2S$ GABA_A receptors. *J Gen Physiol* **131**: 163-181.

Lavoie AM, Twyman RE (1996) Direct evidence for diazepam modulation of GABA_A receptor microscopic affinity. *Neuropharmacology* **35**: 1383-1392.

McKernan RM, Whiting PJ (1996) Which GABA_A-receptor subtypes really occur in the brain? *TINS* **19**: 139-143.

Mellor JR, Randall AD (1997) Frequency-dependent actions of benzodiazepines on GABA_A receptors in cultured murine cerebellar granule cells. *J Physiol* **503**: 353-369.

Mercik K, Piast M, Mozrzymas JW (2007) Benzodiazepine receptor agonists affect both binding and gating of recombinant $\alpha 1\beta 2\gamma 2$ gamma-aminobutyric acid-A receptors. *Neuroreport* **18**: 781-785.

Mozrzymas JW, Barberis A, Mercik K, Zarnowska ED (2003) Binding sites, singly bound states, and conformation coupling shape GABA-evoked currents. *J Neurophysiol* **89**: 871-883.

Perrais D, Ropert N (1999) Effect of zolpidem on miniature IPSCs and occupancy of postsynaptic GABA_A receptors in central synapses. *J Neurosci* **19**: 578-588.

MOL #58289

Revah F, Bertrand D, Galzi JL, Devillers-Thiéry A, Mulle C, Hussy N, Bertrand S, Ballivet M, Changeux JP (1991) Mutations in the channel domain alter desensitization of a neuronal nicotinic receptor. *Nature* **353**: 846-849.

Rogers CJ, Twyman RE, Macdonald RL (1994) Benzodiazepine and β -carboline regulation of single GABA_A receptor channels of mouse spinal neurons in culture. *J Physiol* **475**: 69-82.

Rüsch D, Forman SA (2005) Classic benzodiazepines modulate the open-close equilibrium in a $\alpha_1\beta_2\gamma_{2L}$ γ -aminobutyric acid type A receptors. *Anesthesiology* **102**: 783-792.

Sancar F, Czajkowski C (2004) A GABA_A receptor mutation linked to human epilepsy (γ_2 R43Q) impairs cell surface expression of $\alpha\beta\gamma$ receptors. *J Biol Chem* **279**: 47034-47039.

Sieghart W (1995) Structure and pharmacology of γ -aminobutyric acid_A receptor subtypes. *Pharm Rev* **47**: 181-234.

Sigel E, Buhr A (1997) The benzodiazepine binding site of GABA_A receptors. *TiPS* **18**: 425-429.

Sigworth FJ (1980) The variance of sodium current fluctuations at the node of Ranvier. *J Physiol* **307**: 97-129.

Tan HO, Reid CA, Single FN, Davies PJ, Chiu C, Murphy S, Clarke AL, Dibbens L, Krestel H, Mulley JC, Jones MV, Seeburg PH, Sakmann B, Berkovic SF, Sprengel R, Petrou S (2007)

MOL #58289

Reduced cortical inhibition in a mouse model of familial childhood absence epilepsy. *PNAS* **104**: 17536-17541.

Vicini S, Mienville JM, Costa E (1987) Actions of benzodiazepine and β -carboline derivatives on γ -aminobutyric acid-activated Cl^- channels recorded from membrane patches of neonatal rat cortical neurons in culture. *J Pharmacol Exp Ther* **243**: 1195-1201.

Wagner DA, Czajkowski C (2001) Structure and dynamics of the GABA binding pocket: a narrowing cleft that constricts during activation. *J Neurosci* **21**: 67-74.

Wagner DA, Czajkowski C, Jones MV (2004) An arginine involved in GABA binding and unbinding but not gating of the GABA_A receptor. *J Neurosci* **24**: 2733-2741.

Wallace RH, Marini C, Petrou S, Harkin LA, Bowser DN, Panchal RG, Williams DA, Sutherland GR, Mulley JC, Scheffer IE, Berkovic SF (2001) Mutant GABA_A receptor $\gamma 2$ -subunit in childhood absence epilepsy and febrile seizures. *Nat Genet* **28**: 49-52.

MOL #58289

Footnotes

[†]This project was supported by the American Epilepsy Society and the Lennox Trust Fund; and the National Institutes of Health [Grant NS046378].

[‡]Authors contributed equally.

Department of Physiology, University of Wisconsin, Madison, Wisconsin 53706 USA (MGO, MVJ)

Department of Biological Sciences, Marquette University, Milwaukee, Wisconsin 53201 USA (DAW)

Howard Florey Institute, University of Melbourne, Parkville 3010, AUS (SP)

MOL #58289

Legends for Figures

Figure 1. Mutations at γ_2 R43, γ_2 E178 or β_2 R117 to lysine (K) or glutamine (Q) enhance desensitization and/or slow deactivation. A) Homology model of the GABA_A receptor (Cromer et al., 2002) illustrating the five subunit ring arrangement. View is from the extracellular side looking through the central channel into the cell. Intersubunit interfaces mediating GABA or BZD binding, or containing the mutated residues, are labeled. B) Zoomed in view of a putative three-residue salt-bridge network linking the γ_2 and β_2 subunits. C-E) Normalized current responses from outside-out patches to rapid application of 10 mM GABA. Traces above current responses in (C) are liquid junction currents obtained with an open pipette tip by blowing off the patch following the experiment to assay the speed of solution exchange. All four γ_2 subunit mutations (C-D) enhanced the rate and/or extent of desensitization during 500 ms pulses (right), whereas only mutations to glutamine significantly slowed deactivation following 2-5 ms pulses (left). The β_2 subunit mutation β_2 R117K slowed deactivation with little effect on desensitization (E). F) Summary of weighted time constants for desensitization and deactivation, and the final extent of desensitization after 500 ms. Differences from $\alpha_1\beta_2\gamma_2$ were evaluated by one-way ANOVA with post-hoc Dunnett's test at * $p < 0.05$ or ** $p < 0.01$.

Figure 2. Mutations at γ_2 R43, γ_2 E178 or β_2 R117 do not preclude γ_2 subunit incorporation into functional receptors. A) Normalized current responses to 2-5 ms (left) and 500 ms (right) pulses of 10 mM GABA for $\alpha_1\beta_2\gamma_2$ and $\alpha_1\beta_2$ receptors (black) and weighted mixtures of those responses simulating currents from a heterogeneous receptor population containing 10-90% $\alpha_1\beta_2$ receptors in 10% increments (thin light gray). The contribution of $\alpha_1\beta_2\gamma_2$ and $\alpha_1\beta_2$ receptors to the resulting current was also weighted by their relative conductances of 33 pS and 11 pS, respectively. Responses from $\alpha_1\beta_2\gamma_2$ R43Q receptors are included for comparison (thick dark gray). B) Effect

MOL #58289

of zinc on GABA-evoked peak responses. Responses to 10 mM GABA were averaged from interleaved recordings with (gray) and without (black) 10 μ M zinc. When present, zinc was both pre- and co-applied for each GABA pulse, which lasted at least 10 ms. Zinc greatly reduced peak currents from $\alpha_1\beta_2$ receptors, but did not affect any of the mutants to a similar degree, suggesting that they form functional receptors incorporating a γ_2 subunit (Hosie et al., 2003). C) Summary of the reduction in peak current by 10 μ M zinc. Differences from $\alpha_1\beta_2$ and $\alpha_1\beta_2\gamma_2$ were evaluated by one-way ANOVA with post-hoc Dunnett's test at $p < 0.01$.

Figure 3. The mutation γ_2 R43Q does not affect maximal open probability (P_{o-max}) or single channel conductance. A) Mean (below) and variance (above) of consecutive responses to 500 ms pulses of 10 mM GABA for $\alpha_1\beta_2\gamma_2$ and $\alpha_1\beta_2\gamma_2$ R43Q receptors. B) Plots of normalized mean current versus variance for $\alpha_1\beta_2\gamma_2$ (black squares) and $\alpha_1\beta_2\gamma_2$ R43Q (gray circles) for the traces shown in (a) fit with a parabola (black line) describing the single channel conductance, P_{o-max} and the number of channels present in each patch, none of which differed between constructs (two-tailed unpaired Student's t -test, $p \leq 0.05$).

Figure 4. Kinetic modeling demonstrates that the kinetic effects of the mutation γ_2 R43Q can be explained by faster channel closure, slower recovery from desensitization and slower unbinding. A-B) The Markov models used to simulate GABA responses (U = unbound, B = bound, O = open, D = desensitized; the model in (A) is previously described in Jones et al., 1998). C) Rate constants used to simulate $\alpha_1\beta_2\gamma_2$ and $\alpha_1\beta_2\gamma_2$ R43Q responses to 10 mM GABA for the model in (A) (units are s^{-1} except for GABA binding steps, which are $M^{-1}s^{-1}$). The values of $k_{\pm 1}$, $k_{\pm 2}$, d_2 , r_2 and p are reported as mean \pm SEM because they were allowed to vary while the model was optimized to simultaneously fit 2-5 ms and 500 ms current responses from individual patches (see methods). k_{-2} and r_2 were the only unconstrained rate constants that significantly differed

MOL #58289

when comparing mutant and wild type models (two-tailed unpaired Student's *t*-test, ***p* < 0.01, ****p* < 0.0001). See supplemental data (Fig. S1) for simulations and rate constants for the model in (B). D-E) Current responses (black) evoked by 2 ms (left) or 500 ms (middle) pulses of 10 mM GABA from two individual patches containing $\alpha_1\beta_2\gamma_2$ (D) and $\alpha_1\beta_2\gamma_2$ R43Q (E) receptors overlaid with simulated responses (red). The model qualitatively reproduces the slowing of paired pulse recovery for $\alpha_1\beta_2\gamma_2$ R43Q (E, right) as compared to $\alpha_1\beta_2\gamma_2$ (D, right) observed by Bowser et al. (2002).

Figure 5. Mutations γ_2 R43Q or β_2 R117K speed diazepam (DZ) dissociation from the GABA_A receptor. A) Responses from $\alpha_1\beta_2\gamma_2$, $\alpha_1\beta_2\gamma_2$ R43Q and $\alpha_1\beta_2$ R117K γ_2 receptors to 20-40 ms pulses of sub-maximal (30 μ M) GABA at varying times following washout of 10 μ M DZ. Open tip currents (top) illustrate the solution exchange protocol. The control response (no pre-equilibration in DZ) is offset to the left of each set of traces, and the dashed line indicates its amplitude. Each of the other responses were obtained on separate, interleaved sweeps, and involved first pre-equilibrating for ≥ 1 s in DZ before rapidly switching to a wash solution, allowing DZ to unbind, and assaying the amount of DZ-induced potentiation remaining after varying time intervals. B) The timecourse of potentiation following washout of DZ had a biphasic shape, with a fast rising phase and slower decay. Solid lines are fits to the mean across patches, which are normalized in the inset to show that both $\alpha_1\beta_2\gamma_2$ R43Q and $\alpha_1\beta_2$ R117K γ_2 speed the decay of potentiation by approximately 2-fold. C) Summary of mean and SEMs for the initial and maximal potentiation after DZ washout, and for the decay time constant from biexponential fits to the potentiation timecourse of individual patches. Differences from $\alpha_1\beta_2\gamma_2$ in each case were evaluated with a two-tailed unpaired Student's *t*-test at **p* < 0.05 or ***p* < 0.01.

MOL #58289

Figure 6. Diazepam (DZ) speeds the rise and prolongs the decay of currents from $\alpha_1\beta_2\gamma_2$, $\alpha_1\beta_2\gamma_2$ R43Q and $\alpha_1\beta_2\gamma_2$ R117K receptors. A) Normalized current responses to 20-40 ms pulses of sub-maximal (30 μ M) GABA. Comparison of control (gray) and DZ pre-equilibrated (black) currents, either at the time of maximal DZ-induced potentiation (prolonged decay) or 10 seconds after washout of DZ (almost completely overlaps control response). Insets illustrate the rising phase under the same conditions. Traces are the same as those in Fig. 5A. B) Summary of rise times and the weighted time constant from biexponential fits to deactivation. Graphs include control responses, those immediately following DZ washout (initial), and responses for which DZ had a maximal effect after washout. Differences in control responses between mutants and $\alpha_1\beta_2\gamma_2$ were assayed with a two-tailed unpaired Student's *t*-test at **p* < 0.05 or ***p* < 0.01, whereas for a single receptor type, differences between control and DZ modulated responses were tested with a two-tailed paired Student's *t*-test at †*p* < 0.05, ††*p* < 0.01 or †††*p* < 0.001.

Figure 7. The effects of diazepam (DZ) can be explained by speeding GABA binding and slowing GABA unbinding. A) An extension of the kinetic model shown in figure 4A allowing DZ binding/unbinding from each state (black: DZ-unbound states, blue: DZ-bound states). The rates $k_{\pm DZ1}$ and $k_{\pm DZ2}$ are the same for each set of singly or doubly bound states, respectively, and the rates between DZ-bound states are identical to their DZ-unbound counterparts (transition rates are labeled as in figure 4A) except for the binding and unbinding rates shown in purple, which were allowed to vary, and p^{DZ} and q^{DZ} , which were constrained (see methods). B) Summary of rate constants or their DZ-induced fold change (mean \pm SEM, bold indicates greater than 2-fold change) for fits to sub-maximal GABA responses alone and following washout of DZ. C) Current responses (black) evoked by 20-40 ms pulses of 30 μ M GABA alone (offset left) or at varying times following washout of 10 μ M DZ (right) for $\alpha_1\beta_2\gamma_2$ and $\alpha_1\beta_2\gamma_2$ R43Q receptors overlaid with simulated responses (red). D-E) Expanded view of the fits shown in (C) with the control and

MOL #58289

maximally potentiated responses overlaid and normalized to illustrate the DZ-induced slowing of deactivation and speeding of the rising phase for $\alpha_1\beta_2\gamma_2$ receptors (insets). We reached the same overall conclusions for a similar extension of the model shown in figure 4B (see supplemental data, Fig. S2).

MOL #58289

Table 1. Summary of biexponential fits to macroscopic kinetics of desensitization and deactivation.

| | τ_{fast} (ms) | % τ_{fast} | τ_{slow} (ms) | $\tau_{weighted}$ (ms) | Extent [†] (%) | n |
|--------------------------------|--------------------|-----------------|--------------------|------------------------|-------------------------|----|
| 500ms desensitization | | | | | | |
| $\alpha_1\beta_2$ | 17 ± 1* | 69 ± 3** | 156 ± 8* | 57 ± 8** | 64 ± 4** | 12 |
| $\alpha_1\beta_2\gamma_2$ | 12 ± 2 | 38 ± 3 | 217 ± 11 | 142 ± 10 | 41 ± 3 | 27 |
| $\alpha_1\beta_2\gamma_2R43K$ | 9 ± 1 | 57 ± 5** | 215 ± 15 | 95 ± 8** | 60 ± 5** | 8 |
| $\alpha_1\beta_2\gamma_2R43Q$ | 7 ± 1* | 68 ± 2** | 166 ± 10* | 59 ± 5** | 72 ± 3** | 20 |
| $\alpha_1\beta_2\gamma_2E178K$ | 15 ± 3 | 49 ± 3 | 222 ± 20 | 121 ± 15 | 58 ± 5* | 8 |
| $\alpha_1\beta_2\gamma_2E178Q$ | 10 ± 1 | 55 ± 5** | 220 ± 18 | 99 ± 9** | 53 ± 3 | 10 |
| $\alpha_1\beta_2R117K\gamma_2$ | 9 ± 1 | 42 ± 5 | 185 ± 5 | 111 ± 10 | 49 ± 2 | 5 |
| 2-5 ms deactivation | | | | | | |
| $\alpha_1\beta_2$ | 19 ± 1** | 73 ± 3** | 198 ± 10** | 68 ± 6* | n/a | 17 |
| $\alpha_1\beta_2\gamma_2$ | 13 ± 1 | 58 ± 2 | 88 ± 6 | 45 ± 4 | n/a | 24 |
| $\alpha_1\beta_2\gamma_2R43K$ | 16 ± 3 | 53 ± 5 | 112 ± 13 | 59 ± 4 | n/a | 6 |
| $\alpha_1\beta_2\gamma_2R43Q$ | 12 ± 1 | 59 ± 2 | 170 ± 21** | 73 ± 6** | n/a | 17 |
| $\alpha_1\beta_2\gamma_2E178K$ | 16 ± 3 | 51 ± 5 | 115 ± 17 | 62 ± 7 | n/a | 8 |
| $\alpha_1\beta_2\gamma_2E178Q$ | 17 ± 2 | 45 ± 2* | 146 ± 14* | 86 ± 7** | n/a | 9 |
| $\alpha_1\beta_2R117K\gamma_2$ | 14 ± 1 | 41 ± 3* | 130 ± 19 | 83 ± 12** | n/a | 5 |

Mutations at γ_2R43 , γ_2E178 and β_2R117 alter the kinetics of responses from outside-out patches to brief (2-5 ms) and longer (500 ms) pulses of 10 mM GABA. Each mutation either enhanced desensitization, slowed deactivation, or both relative to $\alpha_1\beta_2\gamma_2$ receptors. The kinetics of $\alpha_1\beta_2$ receptors are listed for comparison. Data are mean ± SEM. Differences from $\alpha_1\beta_2\gamma_2$ were

MOL #58289

evaluated by one-way ANOVA with post-hoc Dunnett's test at * $p < 0.05$ or ** $p < 0.01$. †Extent of desensitization at the end of a 500 ms pulse.

Figure 1

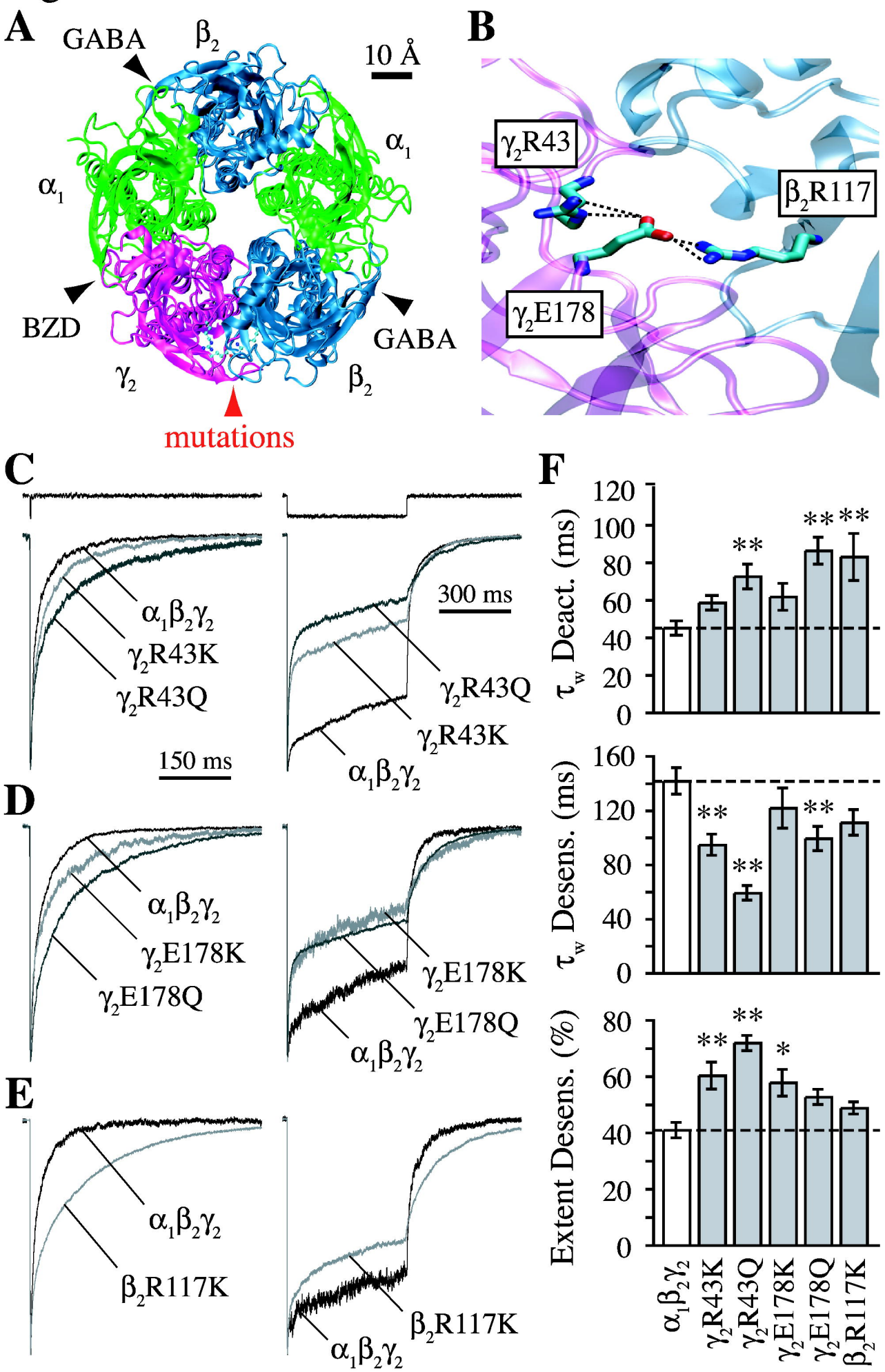
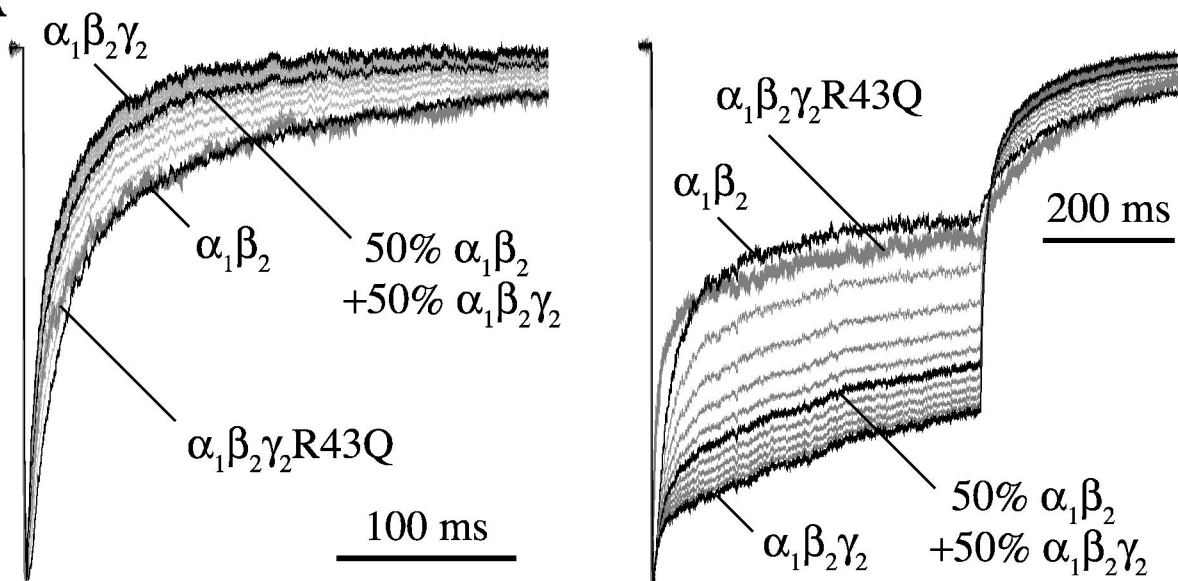
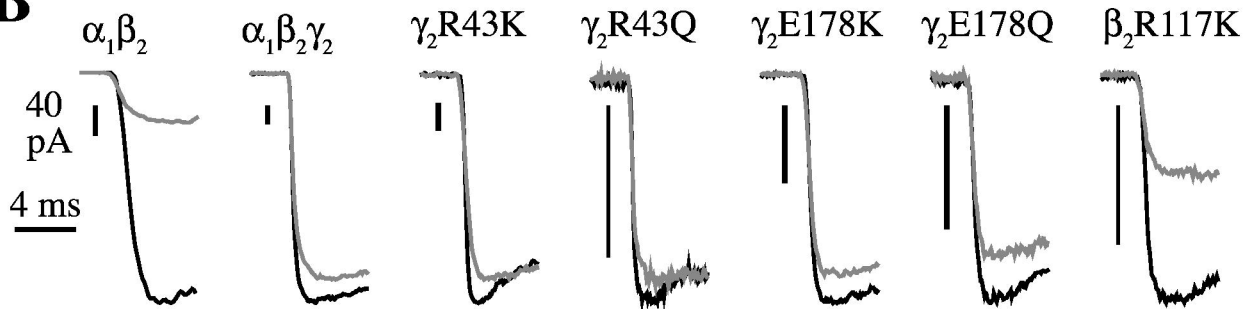


Figure 2

A



B



C

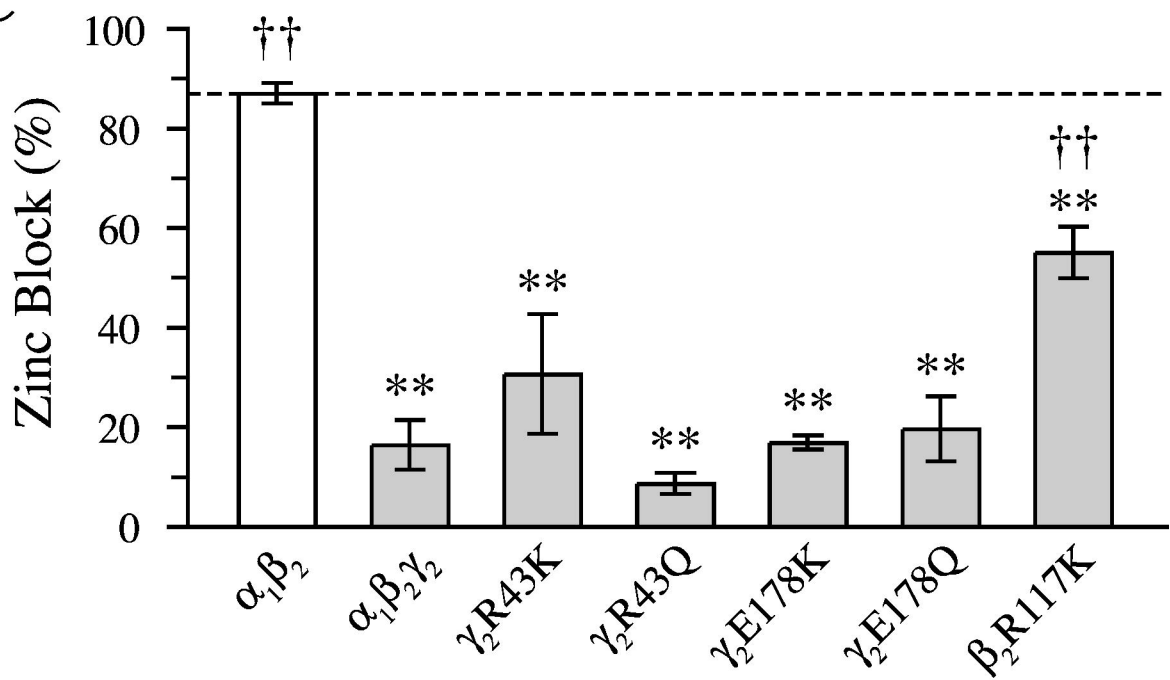


Figure 3

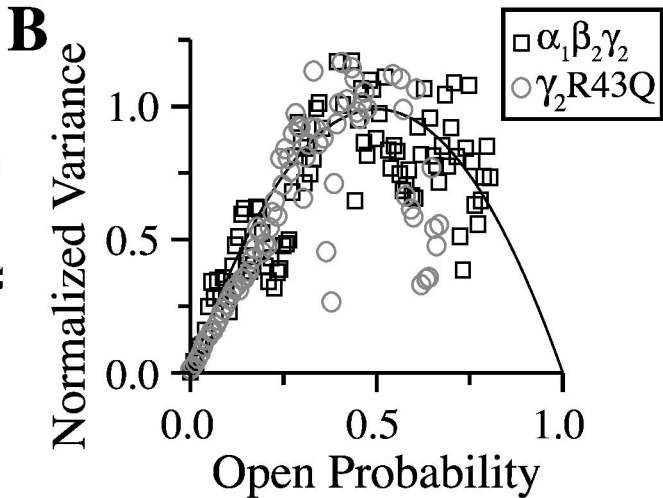
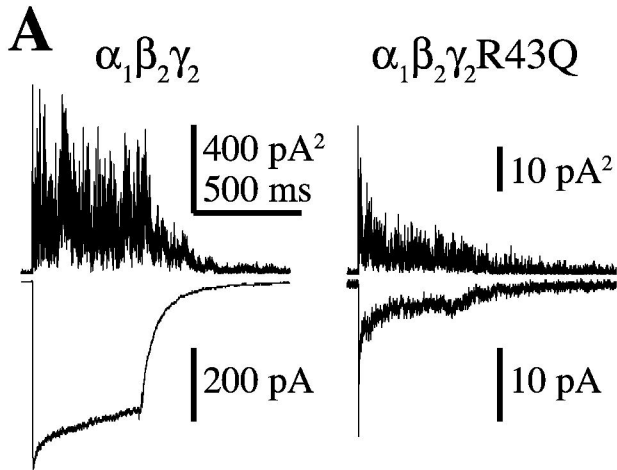
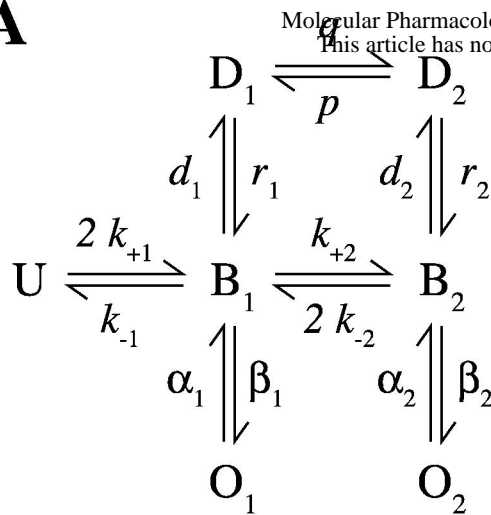


Figure 4

Molecular Pharmacology Fast Forward. Published on October 21, 2009 as DOI: 10.1124/mol.109.058
 This article has not been copyedited and formatted. The final version may differ from this version.

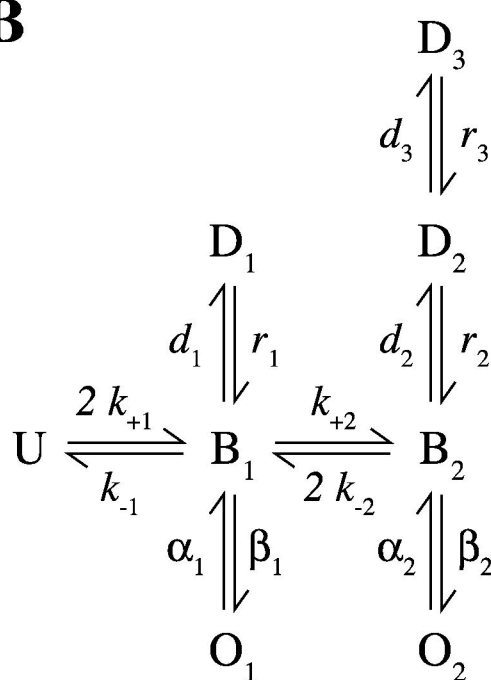
A



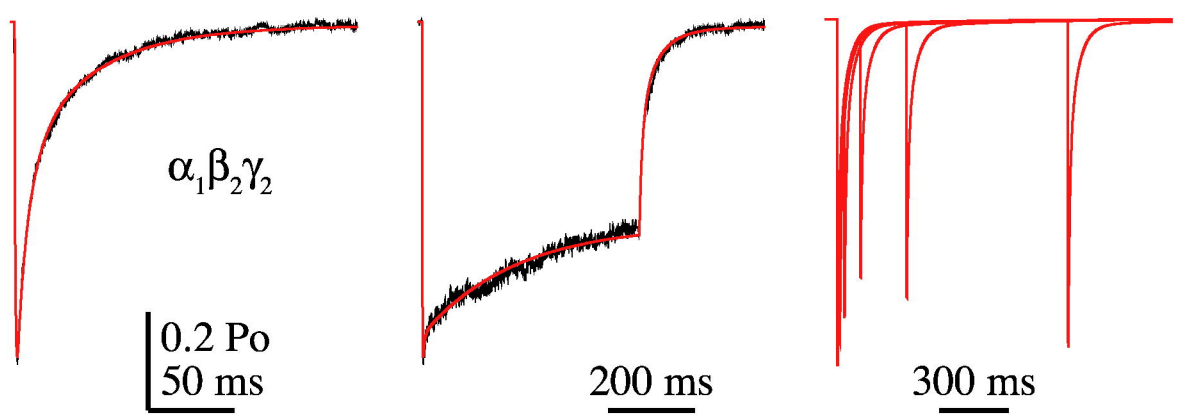
C

| | $\alpha_1\beta_2\gamma_2$ | $\alpha_1\beta_2\gamma_2R43Q$ |
|------------|---------------------------|----------------------------------|
| k_{+1} | $1.9 \pm 0.1 \times 10^6$ | $3.1 \pm 0.9 \times 10^6$ |
| k_{+2} | $1.2 \pm 0.2 \times 10^6$ | $1.0 \pm 0.01 \times 10^6$ |
| k_{-1} | 13 ± 2 | 17 ± 5 |
| k_{-2} | 550 ± 110 | 90 ± 18 ** |
| β_1 | 1000 | 1000 |
| α_1 | 3300 | 3300 |
| β_2 | 2500 | 2500 |
| α_2 | 380 | 570 |
| d_1 | 10 | 10 |
| r_1 | 3 | 3 |
| d_2 | 550 ± 15 | 530 ± 67 |
| r_2 | 150 ± 10 | 60 ± 8 *** |
| q | 0.03 | 0.03 |
| p | 5 ± 1 | 6 ± 1 |

B



D



E

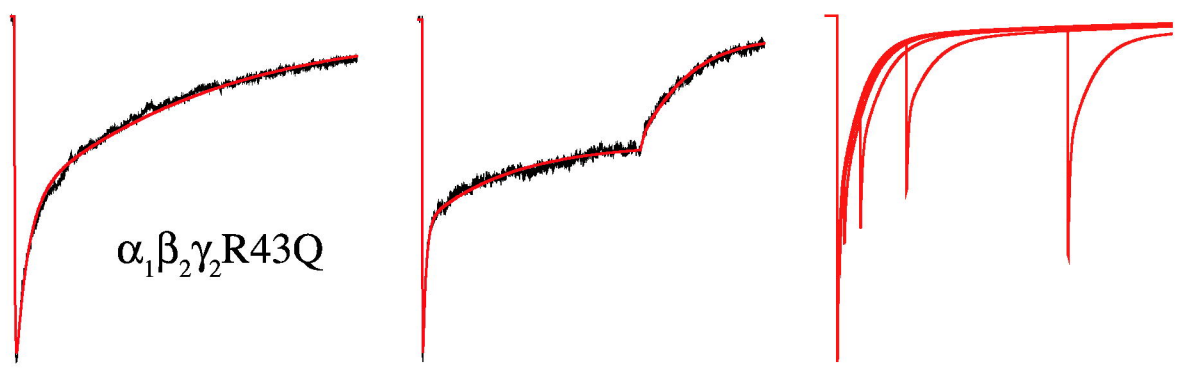


Figure 5

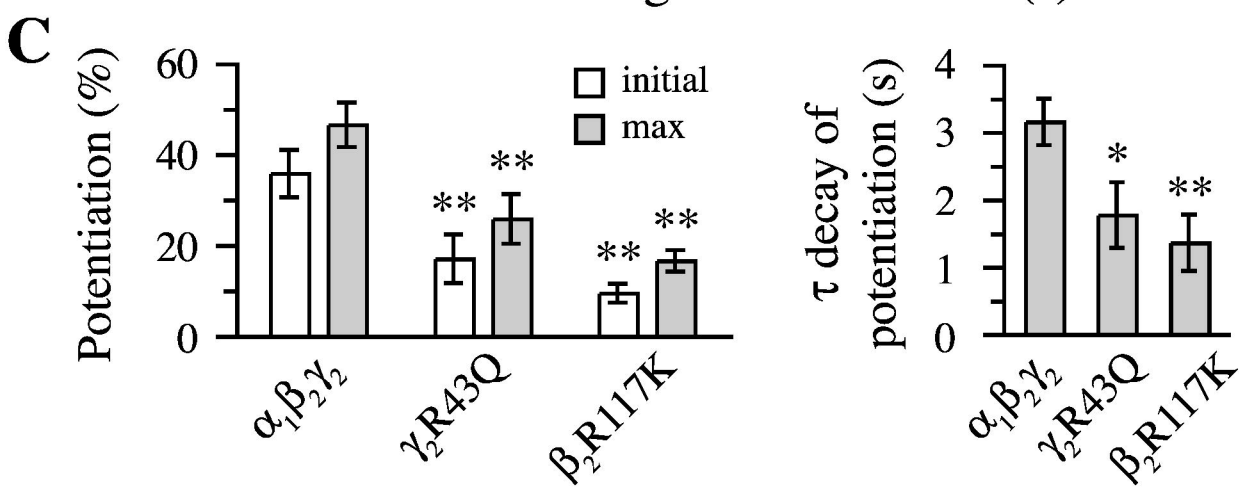
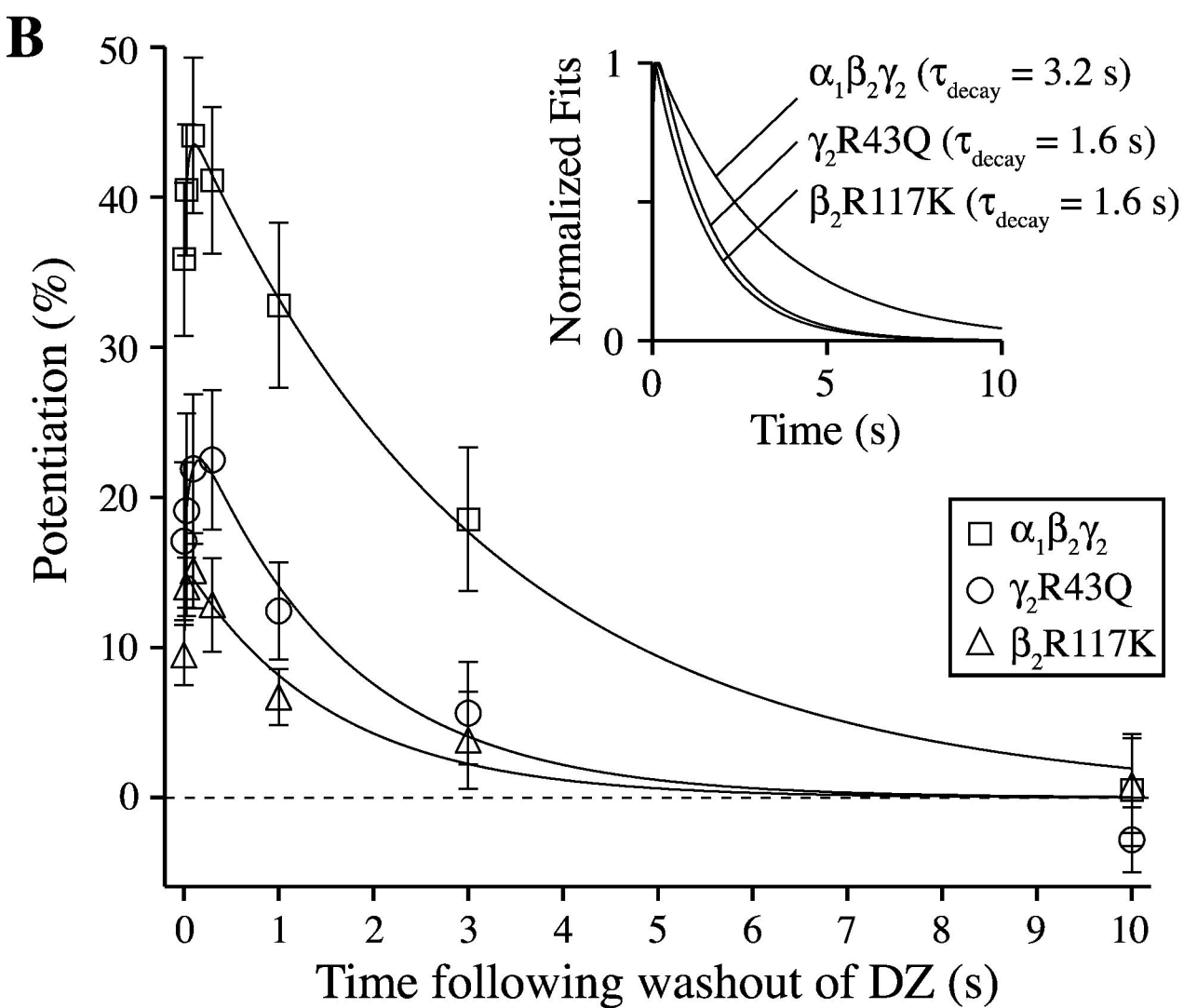
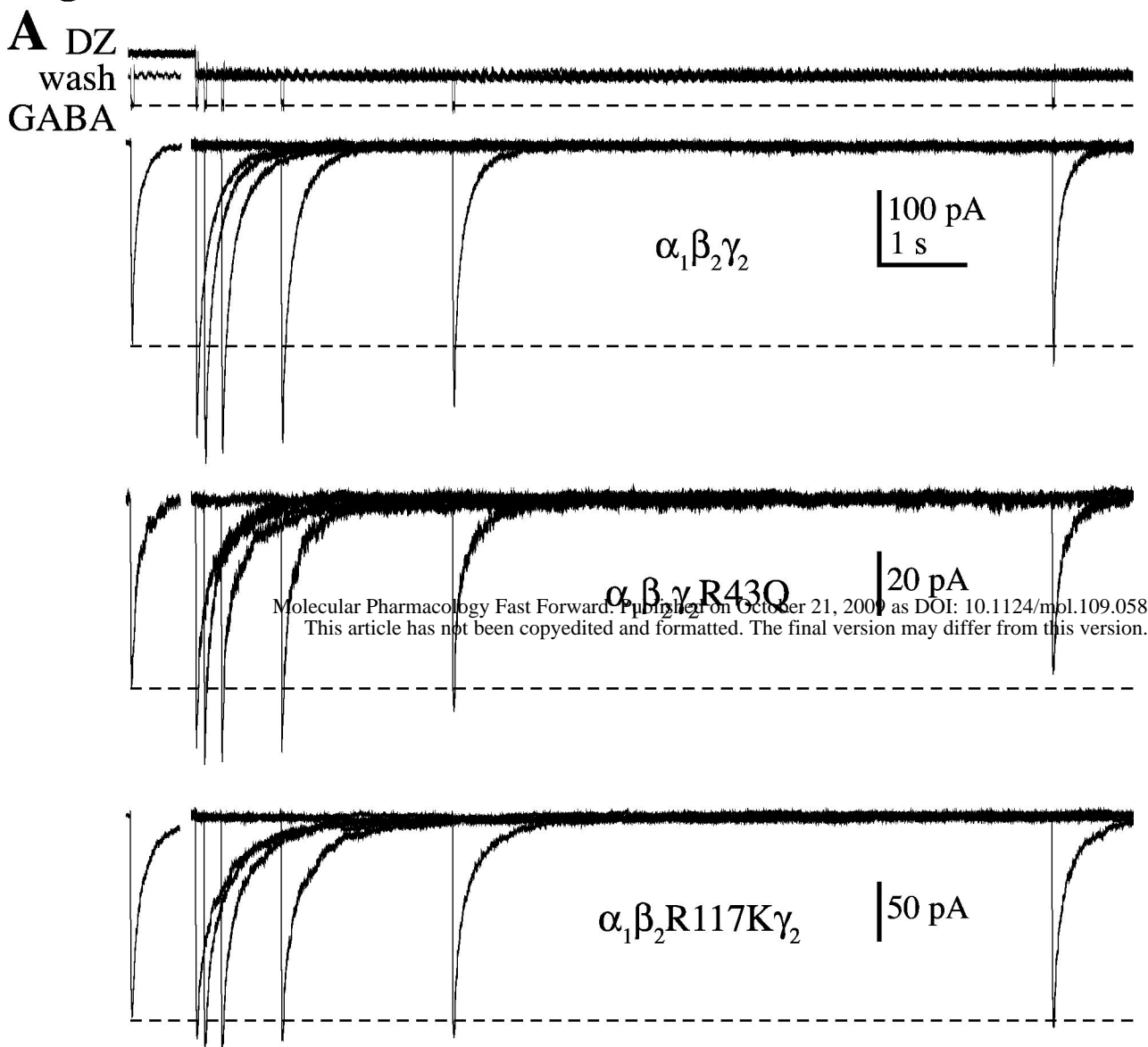


Figure 6

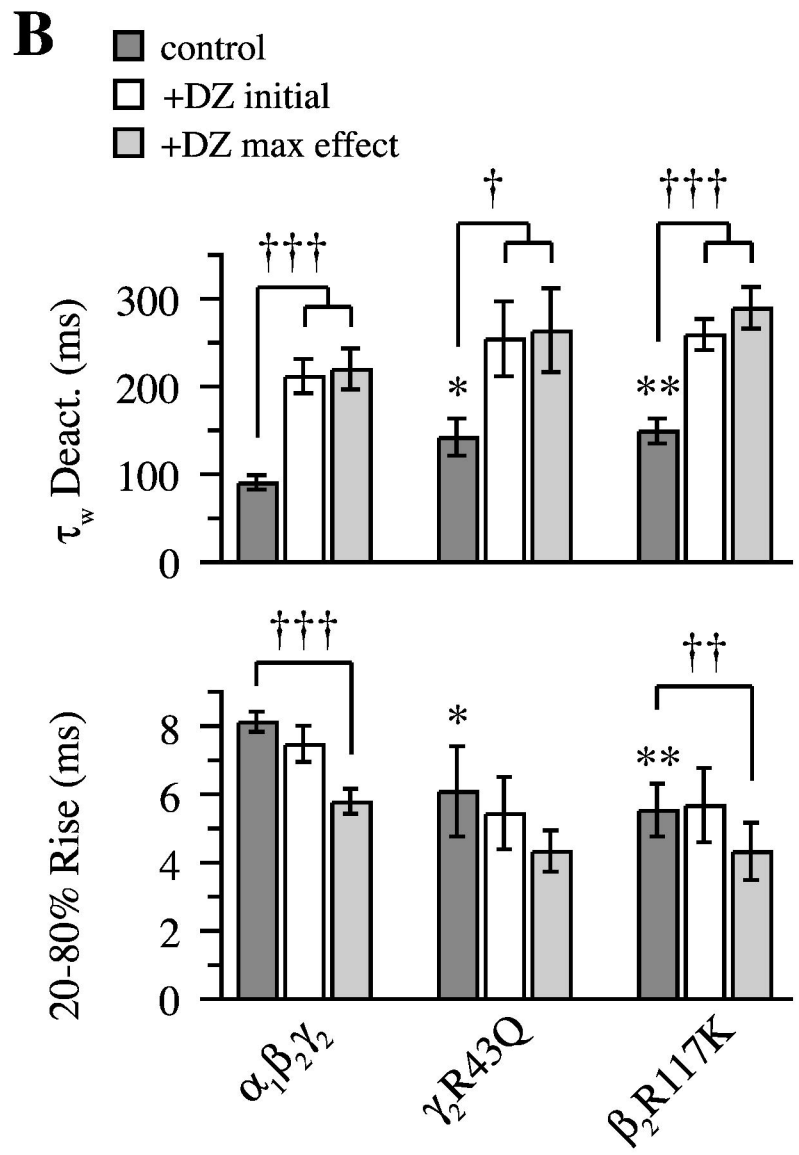
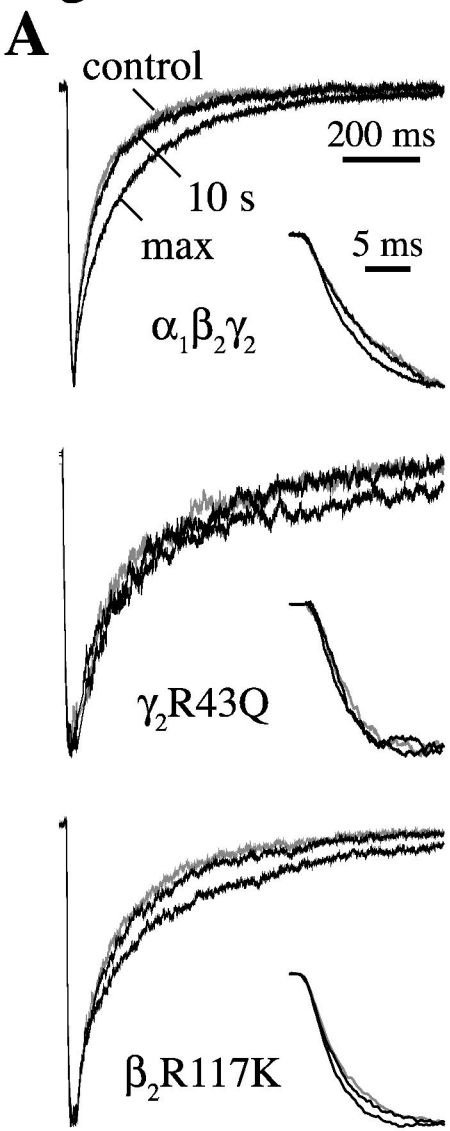
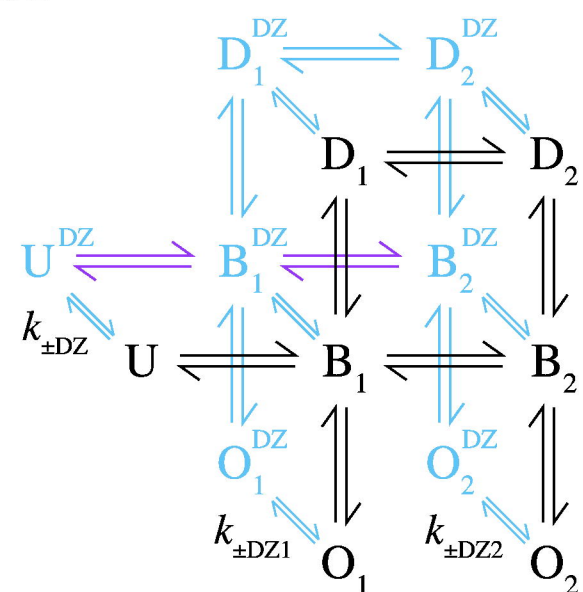


Figure 7

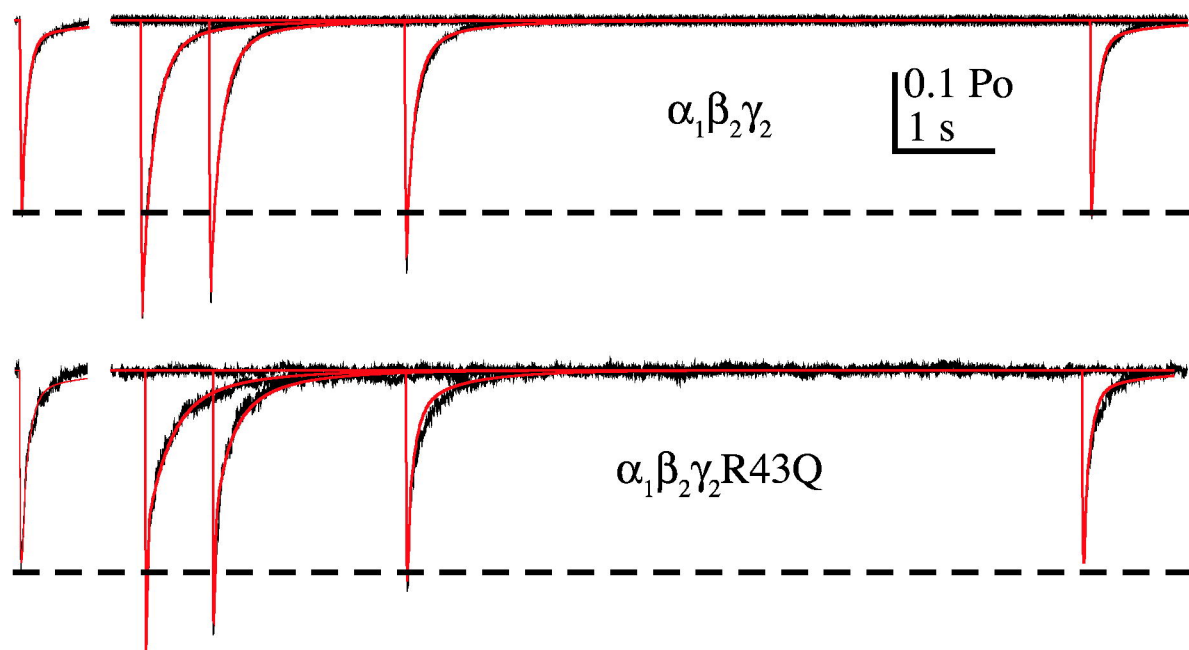
A



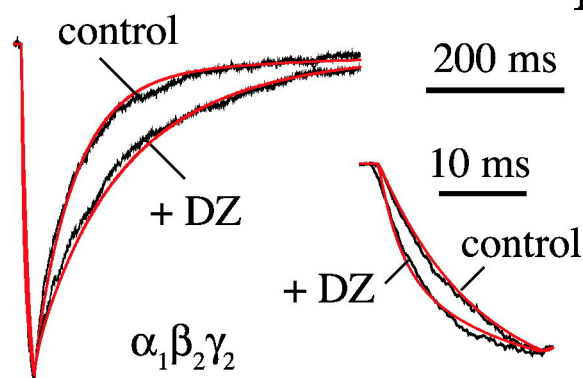
B

| | $\alpha_1\beta_2\gamma_2$ | $\alpha_1\beta_2\gamma_2\text{R43Q}$ |
|------------------------------|----------------------------------|--------------------------------------|
| k_{+DZ} | 1.0×10^8 | 1.0×10^8 |
| k_{+DZ1} | $5.7 \pm 2.0 \times 10^8$ | $1.8 \pm 0.3 \times 10^8$ |
| k_{+DZ2} | $3.0 \pm 1.6 \times 10^9$ | $1.7 \pm 0.9 \times 10^9$ |
| k_{-DZ} | 0.31 | 0.56 |
| k_{-DZ1} | 0.27 ± 0.03 | 0.47 ± 0.04 |
| k_{-DZ2} | 0.20 ± 0.05 | 0.29 ± 0.14 |
| Fold change upon DZ binding: | | |
| k_{+1}^{DZ} | 4.0 ± 0.2 | 1.8 ± 0.3 |
| k_{+2}^{DZ} | 1.7 ± 0.2 | 6.8 ± 2.3 |
| k_{-1}^{DZ} | 0.8 ± 0.3 | 0.9 ± 0.1 |
| k_{-2}^{DZ} | 0.3 ± 0.04 | 0.3 ± 0.05 |

C



D



E

